Journal of Applied Polymer Science

Effect of adhesive thickness on the wettability and deformability of polyacrylic pressure-sensitive adhesives during probe tack test

Nozomi Karyu,[1] Masayo Noda,[1] Syuji Fujii,[1] Yoshinobu Nakamura,[1] Yoshiaki Urahama[2]
[1]Department of Applied Chemistry, Osaka Institute of Technology, 5-16-1 Ohmiya, Asahi-ku, Osaka 535-8585, Japan
[2]Graduate School of Engineering, University of Hyogo, 2167 Shosha, Himeji, Hyogo 671-2201, Japan
Correspondence to: Y. Nakamura (E-mail: nakamura@chem.oit.ac.jp)

ABSTRACT: Effect of adhesive thickness on the wetting and deformation behaviors during probe tack test of pressure-sensitive adhesive (PSA) was investigated. For this purpose, cross-linked poly(*n*-butyl acrylate-acrylic acid) [P(BA-AA)] and poly(2-ethylhexyl acrylate-acrylic acid) [P(2EHA-AA)] random copolymers with an acrylic acid content of 5 wt % and thicknesses in the range of ~15–60 μm were used. Tack was measured using the probe tack test and the fracture energy was calculated from the areas under force–displacement curve recorded during debonding process. From contact time dependence of fracture energy, the rising rate of fracture energy with contact time increased with increasing of adhesive thickness and was P(2EHA-AA) > P(BA-AA). The fracture energy was P(BA-AA) > P(2EHA-AA) at shorter contact time, whereas it reversed at longer contact time. This was caused by two different interfacial adhesions: the physical wetting of PSA molecules to the adherend surface with contact time and the chemical interaction between the acrylic acid units and the adherend surface. From the force–displacement curve measured under the condition of sufficient interfacial adhesion, both maximum force and displacement—namely, the deformability of PSA during debonding process—increased with adhesive thickness. The degree of increase of deformability was P(2EHA-AA) > P(BA-AA). The fracture energy was found to depend on the development of interfacial adhesion during contacting process and the deformability of PSA during debonding process. © 2016 Wiley Periodicals, Inc. J. Appl. Polym. Sci. **2016**, *133*, 43639.

KEYWORDS: adhesives; copolymers; surfaces and interfaces; viscosity and viscoelasticity

Received 4 December 2015; accepted 10 March 2016
DOI: 10.1002/app.43639

INTRODUCTION

The most important feature of pressure-sensitive adhesive (PSA) tape is the ability to adhere to a substrate in response to light pressure and after a short contact time, a property termed "tack." The American Society for Testing and Materials (ASTM) defines tack as "the force required to separate an adherend and an adhesive at the interface shortly after they have been brought rapidly into contact under light load of short duration."[1] The ASTM has specified the light load and the short duration to be 9.8 kPa and 1 s, respectively. In our previous works, however, we have employed alternative conditions as a means of investigating the adhesion mechanism of PSAs.

Tse,[2] Yang,[3] and other researchers[4–6] pointed out that the adhesion strength of a PSA is affected by two factors: the development of interfacial adhesion and the cohesive strength of PSA itself. However, it is difficult to divide these two factors and to analyze separately. Previously,[7] to investigate the influence of interfacial adhesion only, the contact time dependence of the tack was determined with the contact times in the range of 1–30,000 s using a probe tack tester. The cross-linked poly(*n*-butyl acrylate-acrylic acid) random copolymers [P(BA-AA)] with various degrees of cross-linking were used. The relationship between tack and contact time was plotted and the tack values were found to increase with contact time. This increase in tack with contact time was attributed to the wetting rate of PSAs to the probe surface. The increase in the tack with contact time was observed to decrease as the degree of cross-linking of the PSA decreased.

The temperature dependence of the tack was also assessed to discuss the relative contribution of interfacial adhesion and cohesive strength of PSA. Tack was observed to increase with temperature up to a peak value, after which it decreased.[7] This peak value shifted to higher temperatures with increases in the degree of cross-linking. With increases in temperature and/or decreases in cross-linking, the interfacial adhesion will increase while the cohesive strength of the PSA will decrease, such that an optimum value is obtained when the best balance of these two factors is reached. The peak shifted to higher temperature

with the increase in the relative contribution of cohesive strength of PSA.

The contact time dependence of the tack values of P(BA-AA) with various degrees of cross-linking was compared with that for the cross-linked poly(2-ethylhexyl acrylate-acrylic acid) random copolymer [P(2EHA-AA)] employed in our previous study.[8] These copolymers are widely utilized as base PSA materials. The rising in tack with contact time was found to be greater in the case of the P(2EHA-AA) compared to the P(BA-AA). In addition, the P(2EHA-AA) exhibited greater molecular mobility than the P(BA-AA) based on the results of ^{1}H pulse nuclear magnetic resonance (pulse NMR) analyses of un-cross-linked PSAs at 23 °C. This finding explains why the P(2EHA-AA) shows a greater rising in tack with contact time than the P(BA-AA).

In this study, wetting and deformation behaviors during probe tack test for P(BA-AA) and P(2EHA-AA) were investigated using test specimens with a constant cross-linking degree and with different adhesive thicknesses, ranging approximately 15–60 μm. The adhesive thickness influences adhesion strength greatly. Bikerman[9] showed theoretically that peel intensity increased depending on adhesive thickness. Johnston[10] experimentally investigated the effect of adhesive thickness on peel strength and found that peel strength increased with increasing adhesive thickness, but plateaued above a certain adhesive thickness. Previously,[11] we drew the conclusion that the result of Johnston[10] is reasonable from the analysis of the morphology of stringiness during peel test. However, the influence of adhesive thickness on tack properties of PSA is hardly investigated. In our discussion, special attentions are paid to the effect of the cohesive strength of PSA on tack properties. Aforementioned Tse[2] and Yang[3] explained that the cohesive strength of PSA is dependent on its viscoelastic (storage and loss moduli) and mechanical properties. So, in this study, the modulus and deformability during debonding process of PSA are focused on as the cohesive strength. The deformability of PSA was discussed using the force–displacement curve recorded during probe tack test under the condition of sufficient interfacial adhesion.

EXPERIMENTAL

Materials

P(BA-AA) with an AA content of 5 wt % [weight average molecular weight (M_w) of 500,000, polydispersity of 4.9, 40 wt % ethyl acetate solution, Toagosei Co., Ltd., Tokyo, Japan] and P(2EHA-AA) with an AA content of 5 wt % (M_w of 490,000, polydispersity of 4.1, 50 wt % ethyl acetate solution, Fujikura Kasei Co., Ltd., Tokyo, Japan) were used as the base polymers. *N*,*N*,*N*′,*N*′-tetraglycidyl-*m*-xylenediamine (Tetrad-X, Mitsubishi Gas Chemical Company, Inc., Tokyo, Japan) was used as a cross-linker. Reagent-grade ethyl acetate was employed throughout.

Sample Preparation

In each preparation, a predetermined quantity of the base polymer solution was mixed with the cross-linker (at a level of 0.008 equivalents, Eq.) together with a quantity of ethyl acetate sufficient to obtain the desired concentration of 40 wt %. Each solution was used to coat a PET film substrate (thickness: 38 μm) serving as an applicator. The cast films were subsequently heated at 115 °C for 2 min to evaporate the ethyl acetate, and then heated at 30 °C for 10 days to accelerate the cross-linking reaction in the same way as the previous report.[11] Even if heated more, neither the further weight reduction nor the increase in the gel fraction took place. The thicknesses of the resulting PSA layers were measured using a thickness indicator (dial thickness gauge H-MT, Ozaki, Tokyo, Japan) and the sample thicknesses were determined to be approximately 15, 30, 45, and 60 μm.

Tensile Properties

The adhesive films cast on a silicone release agent-coated PET film were cut into squares (50 × 50 mm) and peeled off. The ~50 μm-thick films were rolled to prepare cylindrical samples. The stress–strain curve was recorded using a tensile testing machine (EZ-LX, Shimadzu Corp., Kyoto, Japan) with a chuck distance of 10 mm and a tensile rate of 5 mm s^{-1}. From the curve, the stress at break and the elongation at break were measured. The 100% modulus was calculated from the stress at 100% strain. Each sample was measured at least five times. The data points represent the average values and the top and bottom of the error bars indicate the maximum or minimum values, respectively.

Probe Tack Test

Tack was measured using a probe tack tester (TE-6002, Tester Sangyo Co., Ltd., Saitama, Japan) at various temperatures using a previously reported method.[7,8,12] A schematic of the test procedure and the measurement component of the probe tack tester are shown in Figure 1. The probe was cylindrical (5 mm in diameter) and made of stainless steel. During these trials, a PSA tape sample was attached to a weight (a), which is set on a supporting board (b). The supporting board drops at a displacement rate of 10 mm·s^{-1} upon initiation of the test (c). The weight supplied a compressive stress of 5.0 kPa. As the probe moved up through a hole in the center of the weight, contact was made between the probe and the adhesive tape sample (d). After a predetermined contact time, the supporting board was raised, again at a rate of 10 mm·s^{-1} (equal to the debonding rate), and debonding between the adhesive and the probe took place (e). During which time, the force–displacement curve was recorded. During these measurements, contact times were in the range of 1–30,000 s for the contact time dependency and 30 s for the temperature dependency. The tack value was calculated from the maximum force value in the force–displacement curve, whereas the fracture energy was determined from the area under the curve. In this study, only the fracture energy values are considered. Each sample was measured eight times; the data points represent the average values and the top and bottom of the error bars indicate the maximum and minimum values, respectively, on all the data plots presented herein. All probe surfaces were polished using an abrasive paper (#2000) prior to each test as explained previously.[7]

As noted, to measure the tack under condition of improved interfacial adhesion, the chamber was preheated to 90 °C for 20 min, followed by cooling to the desired measurement

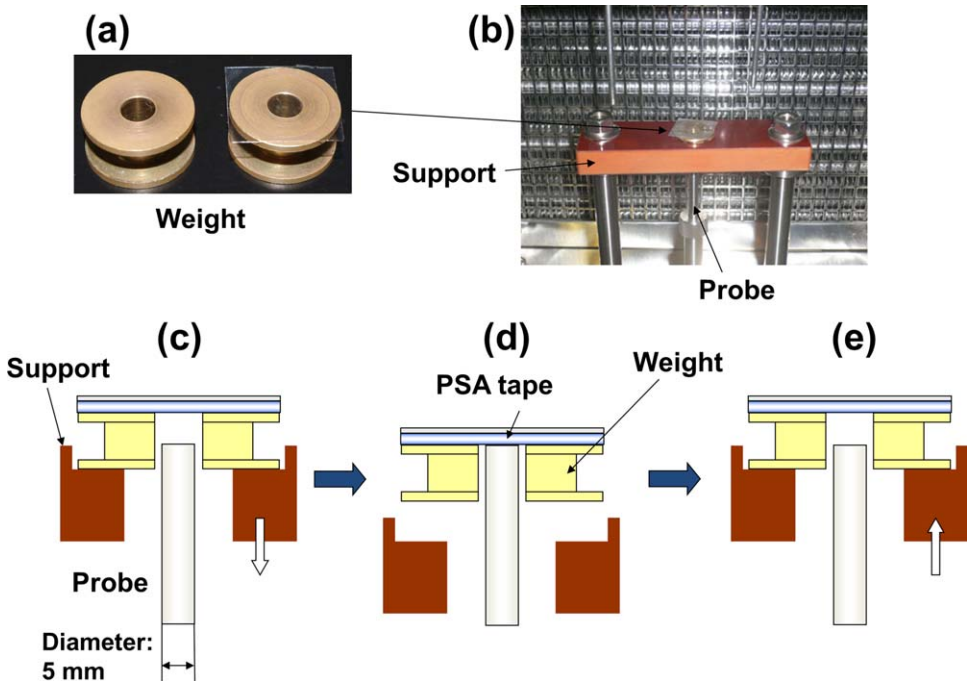

Figure 1. Components of the probe tack tester, including (a) weights and (b) the test apparatus, and diagrams of the test procedure showing (c) the probe prior to sample contact, (d) bonding of the probe to the sample, and (e) debonding. [Color figure can be viewed in the online issue, which is available at wileyonlinelibrary.com.]

temperature over 40 min after contact between the probe and the PSA tape but before initiating debonding. This process is termed "preheating" herein while the standard procedure is denoted as "no heating."

As shown in Figure 1(a), the PSA tape specimen was applied to the top of the weight in our probe tack test. Thus, the tape underwent deformation during debonding process, so that the effect of the deformation of the backing material (the PET film) is also included in the force–displacement curve. To allow measurements of the force–displacement curve of the PSA alone, the PSA tape was applied to a glass plate using a quick-drying adhesive in some trials. This backing is termed "glass-reinforced PET film."

Interfacial Tension

In preparation for interfacial tensions measurements, the ethyl acetate solvent in PSA solution was evaporated completely. The obtained P(BA-AA) and P(2EHA-AA) were dissolved in toluene and the toluene solutions with concentrations in the range from 0.02 to 1 wt % were prepared. The interfacial tensions between these toluene solutions and water were measured using a ring method (the so-called du Noüy method) at 23 °C in conjunction with a surface tensiometer (AN-526P type, Elex Scientific Co., Ltd., Tokyo, Japan).

RESULTS AND DISCUSSION

PSA's 100% Modulus

Figure 2 shows the stress–strain curves for cross-linked P(BA-AA) and cross-linked P(2EHA-AA) measured by the tensile test with a tensile rate of 5 mm s^{-1}. The cross-linker level is 0.008 Eq. The obtained 100% modulus, the stress at break, and the elongation at break were listed in the table at the upper part. The 100% modulus was higher for P(BA-AA) than for P(2EHA-AA). The bulker 2-ethylhexyl groups in P(2EHA-AA) extend the distance between main chains than the *n*-BA groups in P(BA-AA). As a result, the intermolecular interaction between main chains becomes weaker in P(2EHA-AA).

The dynamic mechanical analysis for P(BA-AA) and P(2EHA-AA) with a cross-linker level of 0.24 Eq. was done at a frequency level of 10 Hz. The peak temperatures of tan δ, namely, the glass transition temperatures were −22 °C for P(BA-AA) and −39 °C for P(2EHA-AA). Previously,[8] the pulse NMR analysis for P(BA-AA) and P(2EHA-AA) with no cross-linker was

	100% Modulus	Stress at break	Elongation at break
	kPa	kPa	%
P(BA-AA)	81.2	845	1610
P(2EHA-AA)	28.1	486	1390

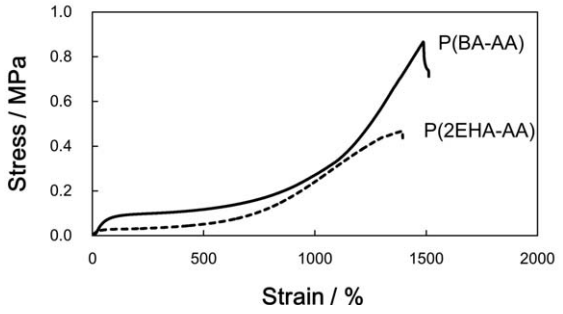

Figure 2. Stress–strain curves of cross-linked P(BA-AA) and cross-linked P(2EHA-AA) made using a cross-linker level of 0.008 Eq. measured by a tensile test.

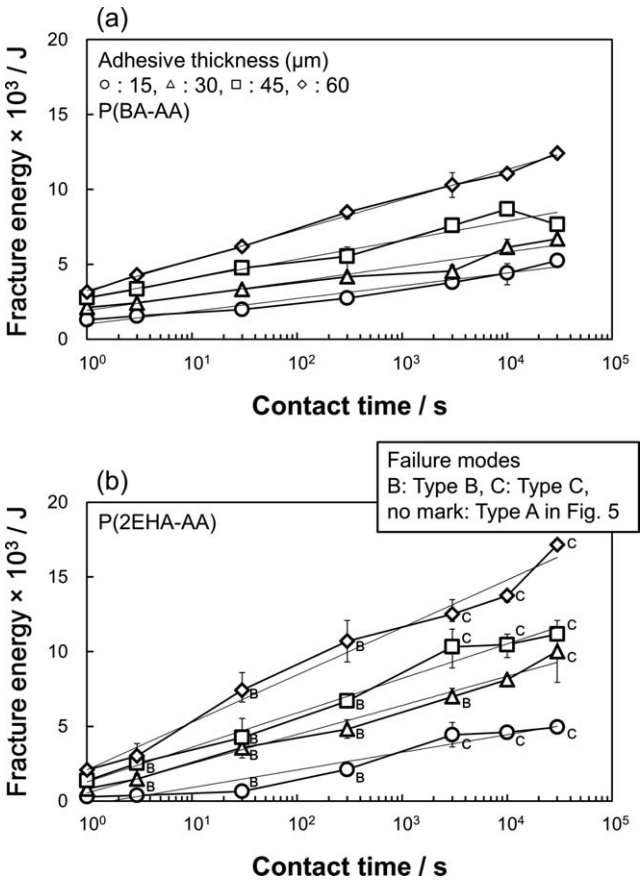

Figure 3. Fracture energy values of (a) cross-linked P(BA-AA) and (b) cross-linked P(2EHA-AA) made with a cross-linker content of 0.008 Eq. as functions of contact time and adhesive thickness as measured by the probe tack test at 20 °C at a debonding rate of 10 mm s^{-1}.

done. The measured result indicated that P(2EHA-AA) has more components with longer relaxation times than P(BA-AA). That is, there are higher molecular mobility components in P(2EHA-AA) than in P(BA-AA). Above results indicate that the cohesive strength level is P(BA-AA) > P(2EHA-AA).

Contact Time Dependency

Zosel[13] suggested that the fracture energy obtained from the area under the force–displacement curve and the shape of force–displacement curve during debonding process are more important than the tack value for understanding the adhesion mechanism. Accordingly, the tack properties were discussed using the fracture energy and the shape of the curve in this study.

Table I. Increasing Rate of Fracture Energy with Contact Time[a]

Adhesive thickness (μm)	The rate of increase of fracture energy[b]	
	P(BA-AA)	P(2EHA-AA)
15	0.37	0.51
30	0.42	0.85
45	0.55	1.00
60	0.88	1.38

[a] The cross-linker content in P(BA-AA) and P(2EHA-AA) is 0.008 Eq. and fracture energy was measured by the probe tack test at 20 °C with a debonding rate of 10 mm·s^{-1}.
[b] The gradient obtained from linear approximation of the relation between fracture energy and contact time shown in Figure 3.

Table II. Interfacial Tension Values at the Water/toluene Interface Subsequent to the Addition of P(BA-AA) or P(2EHA-AA) as Measured Using the du Noüy Ring Method at 23 °C

Concentration (wt %)	Interfacial tension (mN/m)	
	P(BA-AA)	P(2EHA-AA)
0	36.7	
0.02	12.2	15.3
0.10	7.3	14.3
1.00	5.9	12.7

P(BA-AA) and P(2EHA-AA) were dissolved in toluene.

Figure 3 presents the plots of the contact time dependence of the fracture energy values for (a) cross-linked P(BA-AA) and (b) cross-linked P(2EHA-AA) specimens. The fracture energy is seemed to increase with both the contact time and the adhesive thickness. The slopes of the plots of fracture energy against contact time in Figure 3 indicate increases in the fracture energy with prolonged contact time. These slope values were calculated by fitting a linear trendline to each graph, and the resulting data are shown in Table I. These values are attributed to the wetting rate of PSAs to the probe surface as explained previously.[7,8] The rate of increase of the fracture energy was higher for P(2EHA-AA) than for P(BA-AA). That is, the P(2EHA-AA) exhibited superior wetting characteristics compared to the P(BA-AA). The fracture energy was also enhanced with increasing adhesive thickness and the effect was more remarkable in P(2EHA-AA) than in P(BA-AA). The apparent modulus of the adhesive decreases with increasing thickness,[14] because the molecular mobilities near the adherend and the backing surfaces were evidently restrained by these surfaces, and the relative rates of motion of such restrained molecules decrease with increased thickness. Furthermore, the molecular mobility is P(2EHA-AA) > P(BA-AA) from the pulse NMR analysis in the previous report.[8]

In Figure 3, at shorter contact times, the P(BA-AA) exhibits greater fracture energy values than the P(2EHA-AA), whereas

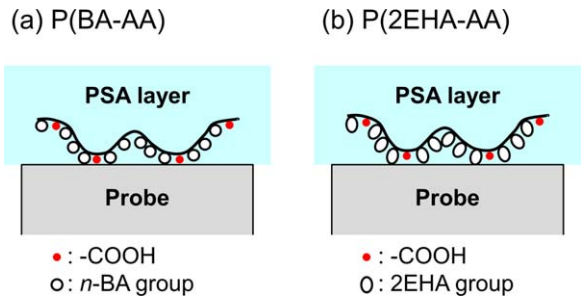

Figure 4. Schematic views of the chemical interaction for (a) P(BA-AA) and (b) P(2EHA-AA). [Color figure can be viewed in the online issue, which is available at wileyonlinelibrary.com.]

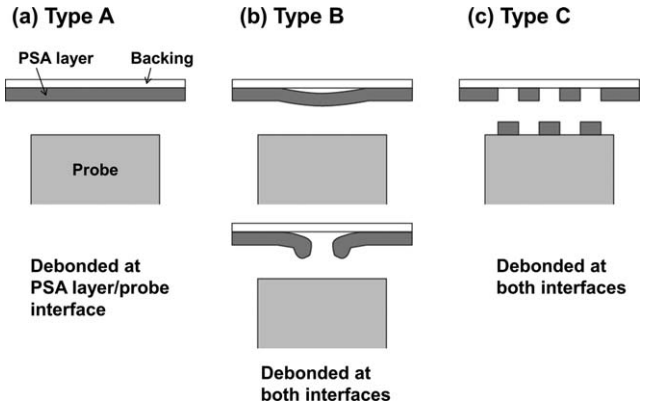

Figure 5. Schematic views of the three different types of failure modes observed following the probe tack test.

the reverse is true at longer contact times. In our previous report,[8] the similar phenomenon was also seen in the comparison of P(BA-AA) and P(2EHA-AA) with the same adhesive thickness and different cross-linker levels. These results suggested that the interfacial adhesion can be divided into two phenomena: the wetting of the probe surface by the PSA molecules (denoted as "physical wetting") and the interactions between the AA units in the PSA and the probe surface (denoted as "chemical interaction"). The physical wetting of P(2EHA-AA) is greater than that of P(BA-AA), and this effect gradually becomes more pronounced with increasing contact time because P(2EHA-AA) has higher molecular mobility than P(BA-AA) as aforementioned. Conversely, the chemical interactions of P(BA-AA) are greater than those of P(2EHA-AA). To confirm this point, the effect of the addition of P(BA-AA) or P(2EHA-AA) on the interfacial tension at the water/toluene interface was measured and are summarized in Table II. The interfacial tension of the pure water/toluene interface was found to be 36.7 mN/m, in good agreement with the literature value of 36.3 mN/m.[15] The addition of P(BA-AA) lowered the interfacial tension more effectively than the addition of P(2EHA-AA). This result indicates that the AA units in the P(BA-AA) molecules will interact with the metal probe surface more effectively compared to those in the P(2EHA-AA). Because the 2-ethylhexyl group is bulkier than the *n*-butyl group, it generates steric hindrance that inhibits the interaction of the AA unit. This comparison is schematically shown in Figure 4. The stronger interactions between the AA units in the P(BA-AA) and the metal surface are thus expected to promote bonding over a shorter contact time. For this reason, the fracture energy was P(BA-AA) > P(2EHA-AA) at shorter contact times, whereas the reverse occurred at longer contact times, as shown in Figure 3. It was also found from Figure 3 and Table I that the adhesive thickness raises the physical wetting preferentially.

All the P(BA-AA) samples summarized in Figure 3 exhibited standard interfacial failure while some P(2EHA-AA) specimens showed abnormal interfacial failure, as shown in Figure 5. The Type A failure shown in this figure occurs when debonding takes place at the probe/PSA layer interface, and represents the typical interfacial failure. In the case of Type B failure, debonding occurs at both the probe/PSA and backing/PSA interfaces. The debonding of the latter interface was typically observed to form a gap, as shown in the upper portion of the Type B diagram. In other cases, however, the PSA layer was ruptured as in the lower portion of the Type B diagram. Type C failures were also observed, in which debonding at both the probe/PSA and backing/PSA interfaces occurred randomly. In Figure 3, the labels "B" and "C" indicate Type B and Type C failures, respectively, while the absence of any label indicates Type A failure. It should be noted that Types B and C failures were observed only for the P(2EHA-AA) specimens (Figure 3). In addition, Types B and C failures occurred preferentially at higher temperatures and when using thicker adhesive specimens, equivalent to those specimens in which the interfacial adhesion was higher. The failure mode observed in the majority of the eight replicate trials is indicated in each figure. The

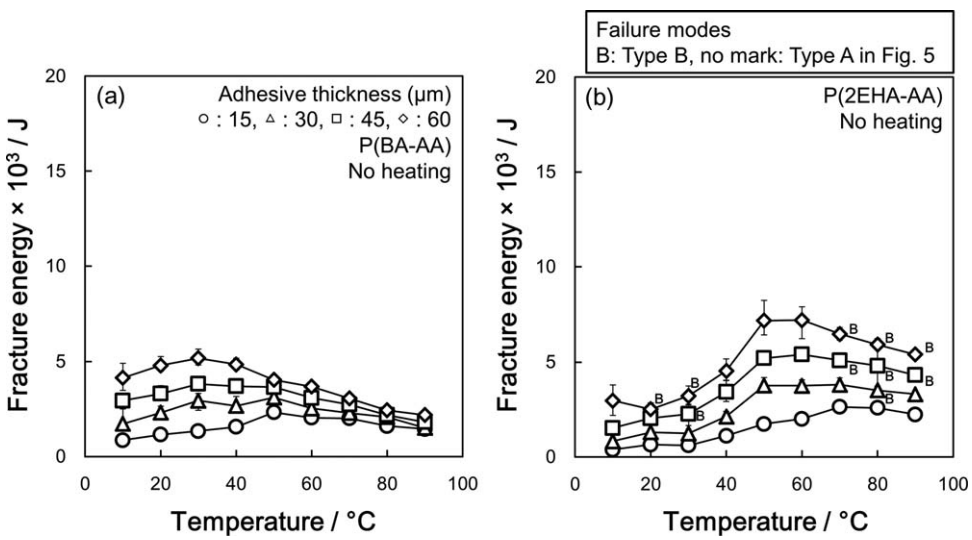

Figure 6. Fracture energy values of (a) cross-linked P(BA-AA) and (b) cross-linked P(2EHA-AA) made with a cross-linker content of 0.008 Eq. as functions of temperature and adhesive thicknesses as measured by the probe tack test under the condition of no heating at a debonding rate of 10 mm s^{-1} and a contact time of 30 s.

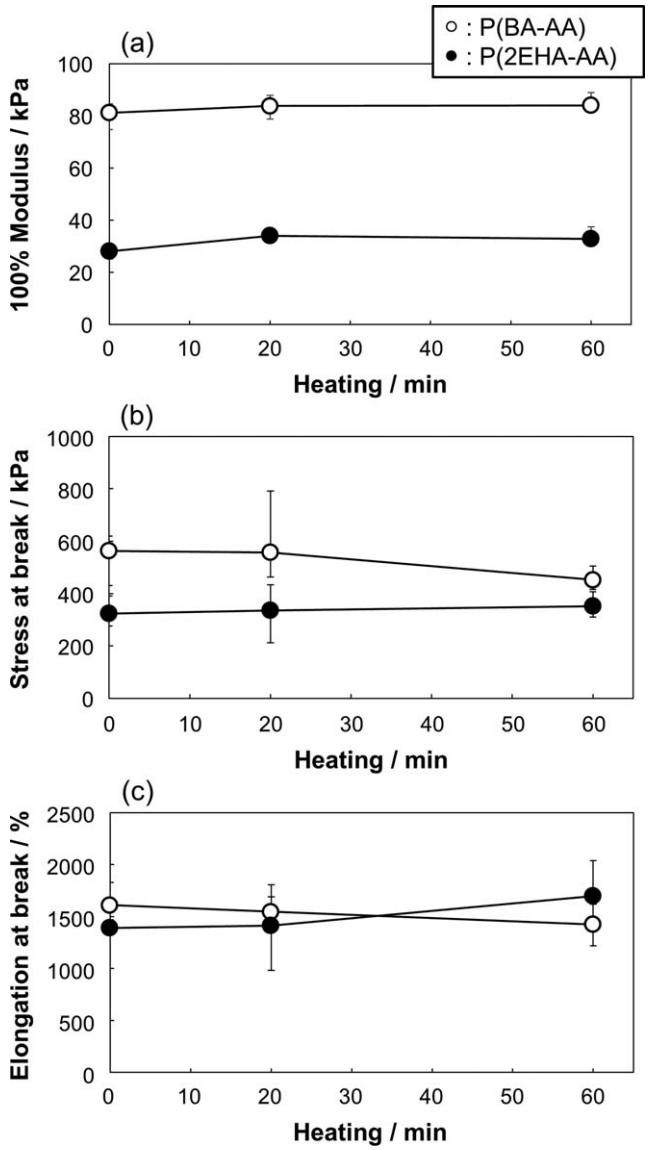

Figure 7. Influence of heating at 90 °C on (a) 100% modulus, (b) stress at break, and (c) elongation at break of cross-linked P(BA-AA) and cross-linked P(2EHA-AA) made using a cross-linker level of 0.008 Eq. measured by a tensile test.

fracture energy values should be shown as the average value by only Type A failure essentially. However, there was no difference between average values by Type A and other failures in Figure 3. So, the fracture energies were shown by the average values containing different failure modes. The same processing was done in Figures (6 and 8), and 13 which will appear later. In the case of commercially available PSA tapes, surface treatment is typically applied to the backing to improve the adhesion properties. For this reason, Type B and C failures are generally not observed with commercial products.

Temperature Dependency

Figure 6 shows the fracture energy values of (a) cross-linked P(BA-AA) and (b) cross-linked P(2EHA-AA) as functions of temperature and adhesive thickness, obtained at a contact time of 30 s. For P(BA-AA) (a), the fracture energy was clearly improved with increasing adhesive thickness especially below 50 °C. The fracture energy increased with temperature before peak and then decreasing. With increases in temperature, the interfacial adhesion will increase while the modulus of PSA will decrease, such that an optimum value is obtained when the best balance of these two factors is reached. The peak temperatures were 50 °C (thicknesses of 15 and 30 μm) and 30 °C (thicknesses of 45 and 60 μm). For P(2EHA-AA) (b), the fracture energy was clearly improved with increasing adhesive thickness; however, it was more remarkable above 50 °C. The peak temperatures were 70 °C (thicknesses of 15 and 30 μm) and 60 °C (thicknesses of 45 and 60 μm). The peak temperatures were higher than those for P(BA-AA).

In Figure 6, it is clear that the fracture energy is P(BA-AA) > P(2EHA-AA) at lower temperature, whereas the reverse occurred at higher temperatures. These phenomena are also caused by the two kids of interfacial adhesion: the physical wetting and the chemical interaction. At lower temperatures, the chemical interaction formed in a shorter contact time (30 s) for P(BA-AA). On the other hand, the appearance of physical wetting was accelerated by heating for P(2EHA-AA). Further, the adhesive thickness raises the physical wetting preferentially. So, the fracture energy of P(2EHA-AA) at higher temperature was improved, and the effect became more remarkable with increasing of adhesive thickness.

The tack test contact time specified by ASTM[1] is 1 s. However, in this study, we employed a contact time of 30 s in the same manner as previous studies[7,8,12] because more reproducible results were obtained at contact times above 10 s. In our previous studies, tack values were determined at a contact time of 1 s[4] and it was found that there were no differences in the basic trends between the results obtained with contact times of 1 and 30 s.

Deformability of PSA

In Figure 5, the interfacial adhesion develops, whereas the modulus of PSA decreases with temperature rising. To discuss the influence of modulus of PSA with temperature rising, the probe tack test under the condition of sufficient interfacial adhesion is desirable. For this purpose, Creton *et al.*[16] employed the thick adhesive layers on the order of 200 μm and applied the significant pressure to the PSA during the contacting process. In this study, we performed the probe tack test with developed interfacial adhesion under the condition of preheating. Under this condition, the sample tape contacted with probe was heated at 90 °C for 20 min followed by cooling to the desired measurement temperature over 40 min, and then the debonding process was started. However, it is desirable that the heating improves only the interfacial adhesion and never influences on the modulus of PSA. To confirm this point, the tensile properties of PSA after heating at 90 °C were measured.

Figure 7 shows the influence of heating at 90 °C on the tensile properties of cross-linked P(BA-AA) and cross-linked P(2EHA-AA). Heating hardly influenced (a) 100% modulus, (b) the stress at break, and (c) the elongation at break. Therefore, the heating affected the interfacial adhesion only.

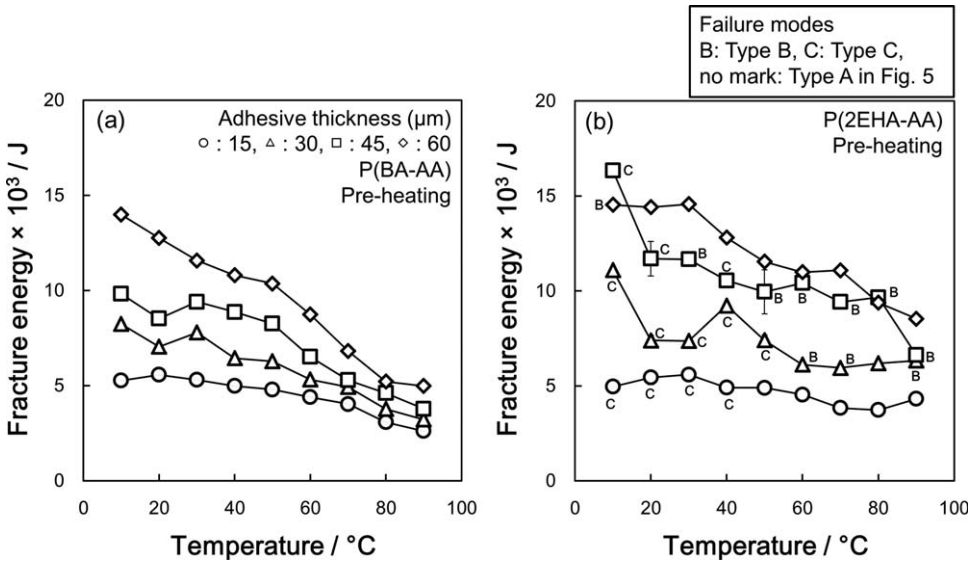

Figure 8. Fracture energy values of (a) cross-linked P(BA-AA) and (b) cross-linked P(2EHA-AA) made with a cross-linker content of 0.008 Eq. as functions of temperature and adhesive thickness as measured by the probe tack test under the condition of preheating at a debonding rate of 10 mm s^{-1}.

The fracture energies measured under the condition of preheating for (a) cross-linked P(BA-AA) and (b) cross-linked P(2EHA-AA) are shown in Figure 8. The fracture energy was evidently lowered with increasing temperature for both systems, such that no peak was observed. These phenomena resulted from the development of interfacial adhesion. Although the interfacial adhesion was improved, an increase in the fracture energy with increasing adhesive thickness was also observed. And the effect of adhesive thickness on the increasing of fracture energy was more significant in (b) P(2EHA-AA) than in (a) P(BA-AA), especially at higher temperature range.

The force–displacement curves during debonding process for (a,c) cross-linked P(BA-AA) and (b,d) cross-linked P(2EHA-AA) of the (a,b) no heating and the (c,d) preheating obtained at 20 °C are presented in Figure 9. In the case of the no-heating specimens (a,b), both the maximum force and maximum displacement were higher for P(BA-AA) than P(2EHA-AA). This is because the chemical interaction formed effectively in the P(BA-AA), in spite

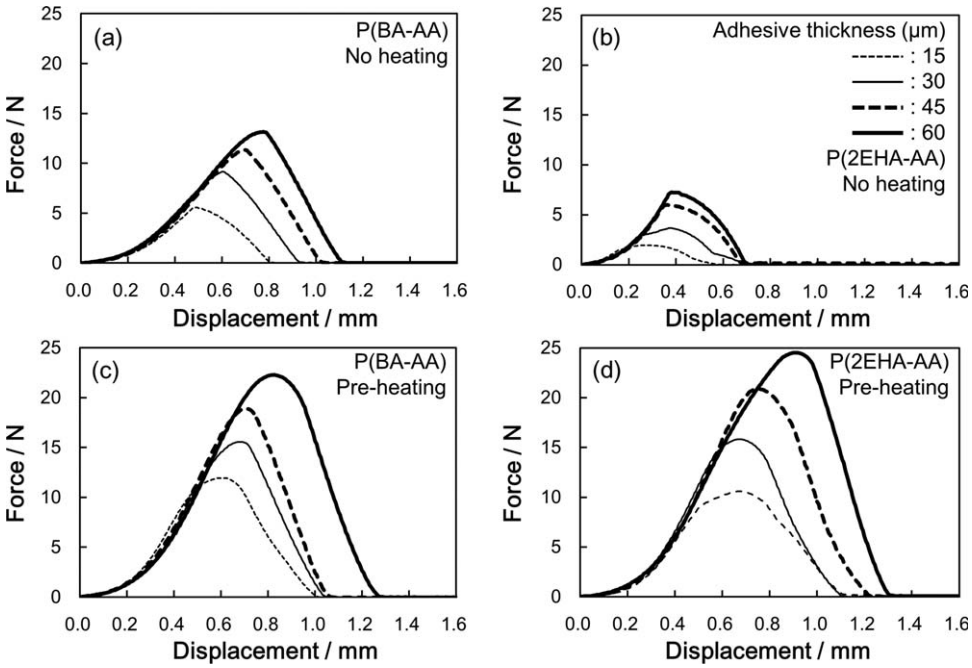

Figure 9. Force–displacement curves obtained from (a,c) cross-linked P(BA-AA) and (b,d) cross-linked P(2EHA-AA) made with a cross-linker content of 0.008 Eq. and with different adhesive thicknesses as measured by the probe tack test at 20 °C under the conditions of (a,b) no heating (contact time of 30 s) and (c,d) preheating at a debonding rate of 10 mm·s^{-1}.

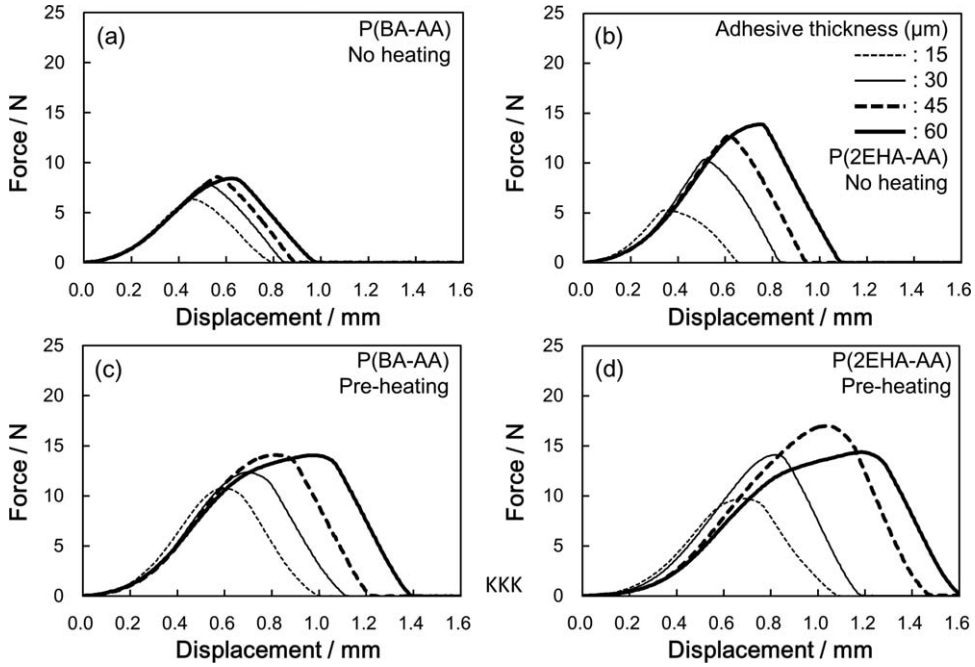

Figure 10. Force–displacement curves obtained from (a,c) cross-linked P(BA-AA) and (b,d) cross-linked P(2EHA-AA) made with a cross-linker content of 0.008 Eq. and with different adhesive thicknesses as measured by the probe tack test at 50 °C under the conditions of (a,b) no heating (contact time of 30 s) and (c,d) preheating at a debonding rate of 10 mm s^{-1}.

of short contact time. So, the maximum displacement seems as the index of interfacial adhesion level. Both the maximum force and the maximum displacement were improved by the preheating for P(BA-AA) (a,c). However, the improvement effect was far remarkable for P(2EHA-AA) (b,d). This is a result of the remarkable improvement in physical wetting as aforementioned.

The same force–displacement curves measured at 50 °C are shown in Figure 10. In the no-heated and preheated P(BA-AA) measured at 50 °C (a,c), the maximum stress was lower than those measured at 20 °C with almost the same maximum displacement [Figure 9(a,c)]. This is caused by the decrease of modulus of PSA with temperature rising. In the no-heated P(2EHA-AA) measured at 50 °C (b), both maximum stress and displacement were higher than that measured at 20 °C [Figure 9(b)]. The physical wetting was improved by temperature rising. In the preheated P(BA-AA) [Figure 9(c)] and P(2EHA-AA) [Figure 9(d)] measured at 20 °C, both the maximum stress and displacement increased with adhesive thickness. On the other hand, the increase in the maximum displacement was more remarkable in those measured at 50 °C [Figure 10(c,d)]. The degree of increase with adhesive thickness of these values in thicker specimen was P(2EHA-AA) > P(BA-AA). From these results, the interfacial adhesion was found to influence on the superior deformability greatly.

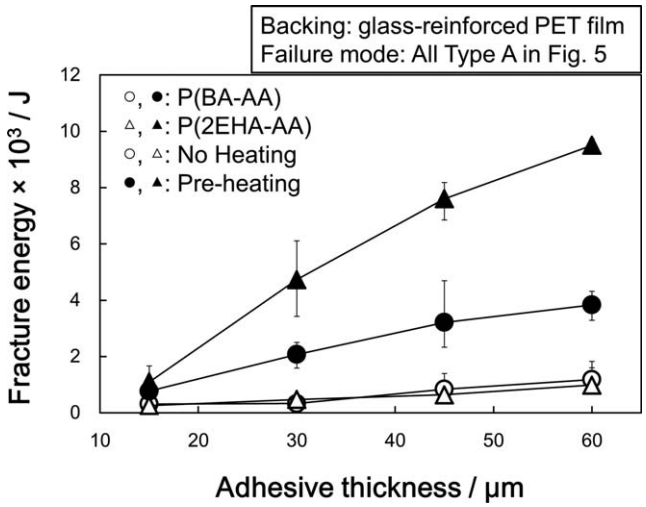

Figure 11. Fracture energy values of cross-linked P(BA-AA) and cross-linked P(2EHA-AA) made with a cross-linker content of 0.008 Eq. as a function of adhesive thickness as measured by the probe tack test at 20 °C under the conditions of no heating (contact time of 30 s) and preheating at a debonding rate of 10 mm·s^{-1}. Backing is glass-reinforced PET film.

As explained in the experimental section, the fracture energy values provided in Figures 3 and 6, and 8 are distorted by the effect of the deformation of the backing material (PET film) to which the PSA tape had been applied. To negate this influence, PSA tape samples were also applied to glass plate substrates using a quick-drying adhesive (the glass-reinforced PET film), following which the tack tests were again performed. The fracture energy values determined by using the glass-reinforced PET film for cross-linked P(BA-AA) and cross-linked P(2EHA-AA) under the conditions of no heating and preheating measured at 20 °C are presented in Figure 11. The fracture energy increased with increasing of adhesive thickness for all systems. There is no difference in the fracture energy between P(BA-AA) and P(2EHA-AA) for no heated system. On the other hand, the fracture energies for P(2EHA-AA) of preheated system were far higher than those for P(BA-AA).

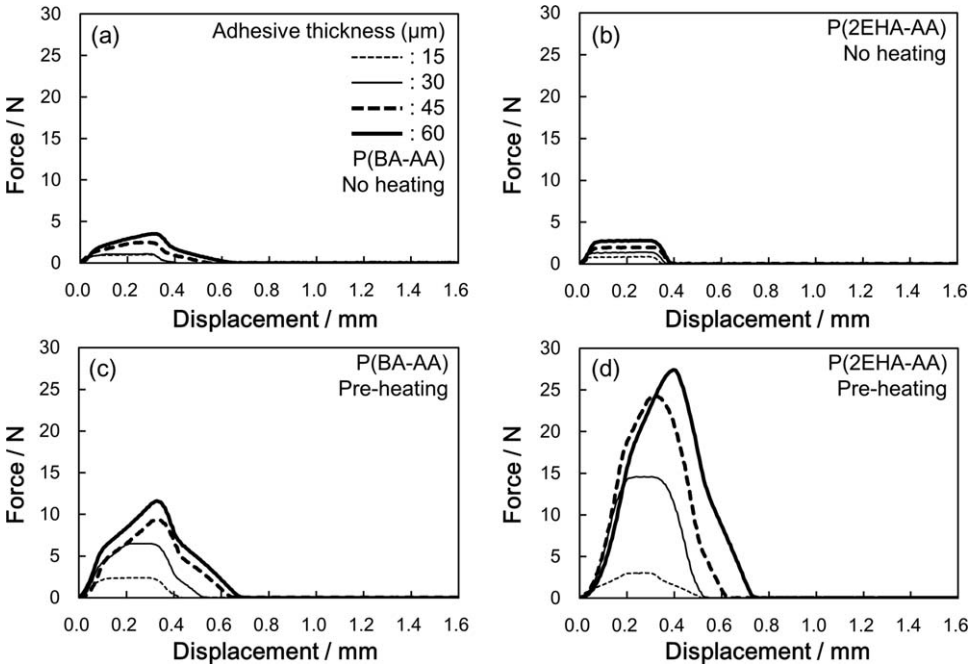

Figure 12. Force–displacement curves obtained from (a,c) cross-linked P(BA-AA) and (b,d) cross-linked P(2EHA-AA) made with a cross-linker content of 0.008 Eq. and with different adhesive thicknesses as measured by the probe tack test at 20 °C under the conditions of (a,b) no heating (contact time of 30 s) and (c,d) preheating at a debonding rate of 10 mm s^{-1}. Backing is glass- reinforced PET film.

The associated force–displacement curves are shown in Figure 12. All maximum stress and displacement values [other than the preheated P(2EHA-AA) with the thicknesses of 45 and 60 μm shown in Figure 11(d)] with the glass-reinforced PET film (Figure 12) were far lower than those with the usual PET film (Figure 9). These are caused by the lower interfacial adhesion in the glass-reinforced PET film system. The PSA tape with usual PET film deforms during the contacting process shown in

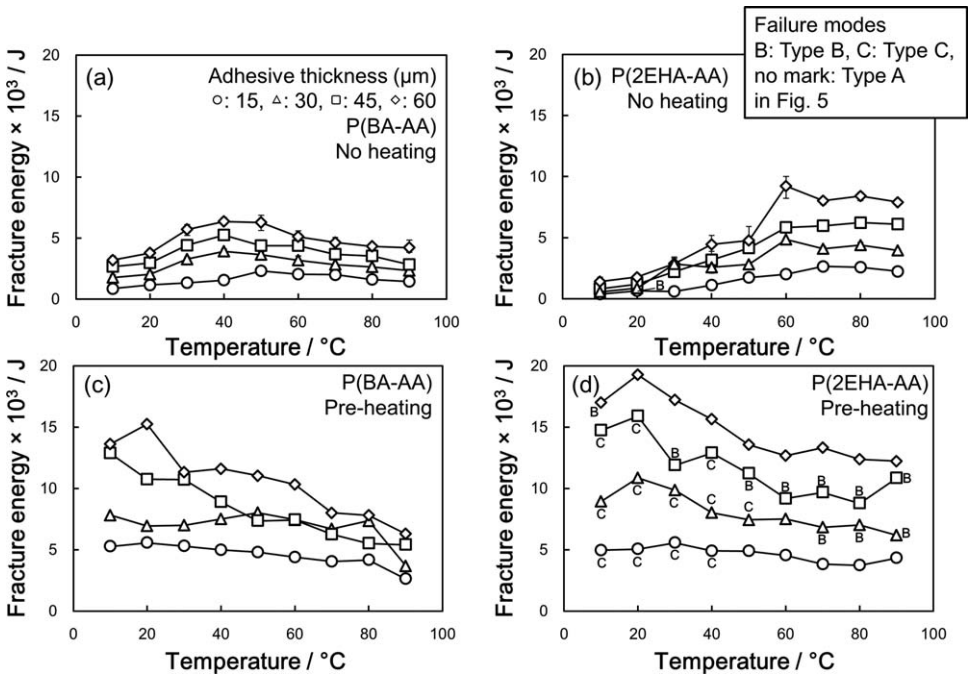

Figure 13. Fracture energy values of (a,c) cross-linked P(BA-AA) and (b,d) cross-linked P(2EHA-AA) made with a cross-linker content of 0.008 Eq. as functions of temperature and adhesive thickness as measured by the probe tack test under the conditions of (a,b) no heating (contact time of 30 s) and (c,d) preheating at debonding rates of 10 (15 μm thickness), 20 (30 μm), 30 (45 μm), and 40 (60 μm) mm s^{-1}. The strain rate is 6.7 × 10^2 s^{-1}.

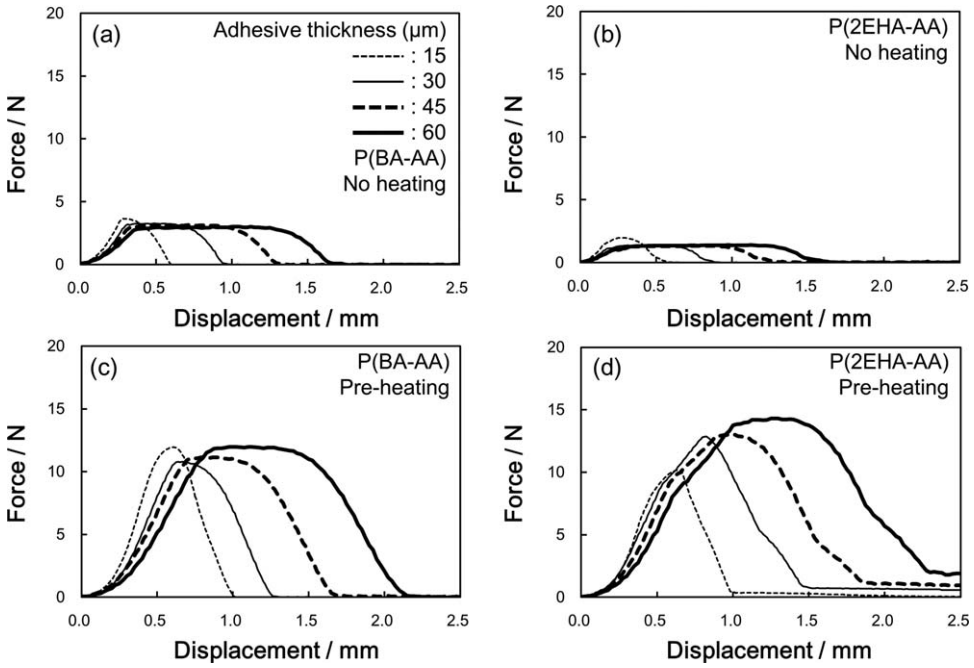

Figure 14. Force–displacement curves obtained from (a,c) cross-linked P(BA-AA) and (b,d) cross-linked P(2EHA-AA) made with a cross-linker content of 0.008 Eq. and with different adhesive thicknesses as measured by the probe tack test at 20 °C under the conditions of (a,b) no heating (contact time of 30 s) and (c,d) preheating at debonding rates of 10 (15 μm thickness), 20 (30 μm), 30 (45 μm), and 40 (60 μm) mm·s^{-1}. The strain rate is 6.7 × 10^2 s^{-1}.

Figure 1(d). This deformation accelerates the wetting of PSA to probe surface, whereas no deformation occurs in the case of glass-reinforced PET film. In the preheated P(2EHA-AA) with the thicknesses of 45 and 60 μm and the glass-reinforced PET film shown in Figure 12(d), the maximum stress values were equal to those with the usual PET film shown in Figure 9(d) although the maximum displacement values were lower. The force–displacement curves of preheated system shown in Figure 12(c,d) indicate the true deformability of PSA, which eliminated the influence of backing material. That is, the true deformability during debonding process seems to be P(2EHA-AA) > P(BA-AA). However, the higher deformability of P(2EHA-AA) is attained by the excellent interfacial adhesion.

Above probe tack test was done under the condition of constant debonding rate. However, the strain rate as actual deformation rate changes with adhesive thickness. To confirm the influence of deformation rate, the probe tack test under the condition of constant strain rate was carried out. The strain rate (r_s) could be determined from the following equation:

$$r_s = \frac{r_d}{a} \quad (1)$$

where r_d is the debonding rate of probe tack test (=10 mm·s^{-1}) and a is the adhesive thickness. The strain rates were 6.7 × 10^2 s^{-1} (adhesive thickness: 15 μm), 3.3 × 10^2 s^{-1} (30 μm), 2.2 × 10^2 s^{-1} (45 μm), and 1.7 × 10^2 s^{-1} (60 μm). Then, the strain rate was unified to 6.7 × 10^2 s^{-1}. The debonding rates under this condition are 10 mm·s^{-1} (adhesive thickness: 15 μm), 20 mm·s^{-1} (30 μm), 30 mm·s^{-1} (45 μm), and 40 mm·s^{-1} (60 μm). The contacting rate is set as 10 mm·s^{-1} for all.

Figure 13 shows the temperature dependence of fracture energy of (a,c) cross-linked P(BA-AA) and (b,d) cross-linked P(2EHA-AA) as functions of temperature and adhesive thickness as measured by the probe tack test under the conditions of (a,b) no heating and (c,d) preheating with a strain rate of 6.7 × 10^2 s^{-1}. The tendencies were similar to the results measured under the condition of constant debonding rate shown in Figures 6 and 8. That is, the rising of the fracture energy with increasing of adhesive thickness was seen clearly.

The force–displacement curves during debonding process under the condition of constant strain rate for (a,c) cross-linked P(BA-AA) and (b,d) cross-linked P(2EHA-AA) of (a,b) the no heating and (c,d) the preheating obtained at 20 °C are presented in Figure 14. The shape of the curves differed as compared with the curve measured under the constant debonding rate (Figure 9). The increase of maximum stress was lowered, whereas the maximum displacement became larger clearly with the increase in adhesive thickness for all the systems. That is, it is clear that the deformability increased with thickness, even under the condition of constant strain rate.

CONCLUSIONS

Wetting and deformation behaviors during probe tack test for cross-linked P(BA-AA) and cross-linked P(2EHA-AA) with different adhesive thicknesses were investigated using the probe tack test. The results of this work indicate the following.

The 100% modulus as the level of cohesive strength measured by tensile test was P(BA-AA) > P(2EHA-AA).

The fracture energy was observed to increase with prolonged contact time and at greater adhesive thicknesses for both P(BA-

AA) and P(2EHA-AA). The wetting rate with increasing of contact time and adhesive thickness was P(2EHA-AA) > P(BA-AA).

The fracture energy order was P(BA-AA) > P(2EHA-AA) at shorter contact times, but this order was reversed at longer contact times. There are two types of interfacial adhesion: the wetting of PSA molecules to the adherend surface (the physical wetting) and the interaction between the acrylic acid units in the PSA molecules with the adherend surface (the chemical interaction). The effect of chemical interaction appears within a short time span and is more important in P(BA-AA). The physical wetting increases gradually with prolonged contact time and is superior in P(2EHA-AA). An increase in the adhesive thickness improves only the physical wetting.

From the temperature dependency, the fracture energy order was P(BA-AA) > P(2EHA-AA) below 40 °C, whereas the reverse was observed above 40 °C. At lower temperatures, the chemical interaction formed for P(BA-AA), whereas the appearance of physical wetting was accelerated at higher temperature for P(2EHA-AA).

From the force–displacement curves measured probe tack test under the conditions of sufficient interfacial adhesion, lowered the deformation of backing and constant strain rate, both maximum force and displacement, namely, the deformability of PSA during debonding process increased with increasing of adhesive thickness. The deformability of PSA under the developed interfacial adhesion was P(2EHA-AA) > P(BA-AA).

Both the interfacial adhesion and the deformability of PSA during debonding process have an effect on tack properties. An increase in the adhesive thickness improves these two factors.

ACKNOWLEDGMENTS

The authors are grateful to the Fujikura Foundation for financial support. The authors also wish to thank the Fujikura Kasei Company and the Toagosei Company for providing the polyacrylic polymer preparations, as well as the Mitsubishi Gas Chemical Company for their kind donation of the cross-linking agent.

REFERENCES

1. ASTM-D2979-01. Standard Test Method for Pressure-Sensitive Tack of Adhesives Using an Inverted Probe Machine **2009**.
2. Tse, M. F. *J. Adhes. Sci. Technol.* **1989**, *3*, 551.
3. Yang, H. W. H. *J. Appl. Polym. Sci.* **1989**, *55*, 645.
4. Zosel, A. *J. Adhes.* **1991**, *34*, 201.
5. Creton, C.; Hu, G.; Deplace, F.; Morgret, L.; Shull, K. R. *Macromolecules* **2009**, *42*, 7605.
6. Tobing, S. D.; Klein, A. *J. Appl. Polym. Sci.* **2001**, *79*, 2230.
7. Nakamura, Y.; Imamura, K.; Yamamura, K.; Fujii, S.; Urahama, Y. *J. Adhes. Sci. Technol.* **2013**, *27*, 1951.
8. Karyu, N.; Shitajima, K.; Fujii, S.; Nakamura, Y.; Urahama, Y. *Int. J. Adhes. Adhes.* **2015**, *60*, 75.
9. Bikerman, J. J. *J. Appl. Phys.* **1957**, *28*, 1484.
10. Johnston, J. *Adhesive Age* **1968**, *11*, 20.
11. Shitajima, K.; Karyu, N.; Fujii, S.; Nakamura, Y.; Urahama, Y. *J. Appl. Polym. Sci.* **2015**, *132*, 8615.
12. Yamamura, K.; Fujii, S.; Nakamura, Y.; Fujiwara, K.; Hikasa, S.; Urahama, Y. *J. Appl. Polym. Sci.* **2013**, *129*, 1008.
13. Zosel, A. In Advances in Pressure-Sensitive Adhesive Technology, 1st ed.; Satas, D., Eds.; Satas & Associates: Warwick, RI, **1992**; Chapter 4, p 92.
14. Takahashi, K.; Shimizu, M.; Inaba, K.; Kishimoto, K.; Inao, Y.; Sugizaki, T. *Int. J. Adhes. Adhes.* **2013**, *45*, 90.
15. Brandrup, J.; Immergut, H., Eds.; Polymer Handbook, 3rd ed.; Wiley: New York, **1989**.
16. Creton, C.; Hooker, J.; Shull, K. R. *Langmuir* **2001**, *17*, 4948.